

integration per minute in a 200-liter container. This value is over six times greater than the upper limit of 0.03 disintegration per minute formed with an unshielded 200-liter container irradiated in the laboratory away from the reactor. Further experiments are to be performed to examine this point. At present it is concluded from our experiments that the cross section for the $\text{Cl}^{37}(\bar{\nu}, e^-)\text{A}^{37}$ reaction is less than 2×10^{-42} cm²/atom for fission product antineutrinos.

An experiment was performed with the 3900-liter tank buried under 19 feet of earth (970 grams/cm²) to explore the possibility of producing A^{37} in the tank by processes other than those associated with the nucleonic component of cosmic radiation. This amount of earth will reduce the intensity of the nucleonic component by a factor of about one thousand. The amount of A^{37} activity in the buried tank was found to be less than 0.05 disintegration per minute at saturation, a limit set by the sensitivity of the counter used. The limit corresponds to detecting 70 neutrino captures per day in the 3900-liter tank. Since the 3900-liter tank with its associated counters was more sensitive for detecting neutrinos than any previously reported device, it is of interest to consider the possibility of detecting neutrinos from the sun. Two processes are now considered im-

portant for energy production in the sun, the proton-proton chain and the carbon-nitrogen cycle.⁷ The neutrinos from the proton-proton chain have a maximum energy (0.41 Mev) below the threshold of 0.816 Mev for the $\text{Cl}^{37}(\nu, e^-)\text{A}^{37}$ reaction and therefore neutrinos from this chain could not be detected by this method. The neutrinos in the carbon-nitrogen cycle arise from the positron decays of N^{13} and O^{15} which have maximum neutrino energies of 1.24 and 1.68 Mev respectively. Based upon this cycle, the flux of neutrinos at the surface of the earth is approximately 6×10^{10} neutrinos/cm² sec.⁸ The estimated average cross section for these neutrinos is about 3×10^{-46} cm² for the reaction. The experiment with the buried 3900-liter tank sets an upper limit on the neutrino flux from the sun of 1×10^{14} neutrinos/cm² sec if the energy production of the sun is entirely through the carbon-nitrogen cycle.

ACKNOWLEDGMENT

The author is indebted to Dr. Byron E. Cohn and Dr. Mario Iona of the University of Denver for their generous assistance in the irradiation carried out on the summit of Mt. Evans.

⁷ E. E. Salpeter, *Ann. Rev. Nuc. Sci.* **2**, 41 (1953).

⁸ F. G. Houtermans and W. Thirring, *Helv. Phys. Acta* **27**, 81 (1954).

Interactions of the Heavy Nuclei of the Cosmic Radiation*

J. H. NOON AND M. F. KAPLON
University of Rochester, Rochester, New York

(Received August 17, 1954)

Fragmentation probabilities have been obtained for the interactions of heavy nuclei with target nuclei of photographic emulsion and a light element absorber (gelatin and cellulose acetate). The predictions of a simple geometrical model for the fragmentation probabilities in light elements derived from those observed in emulsion are in agreement with experimental observations. Measurements of the interaction mean free paths of heavy nuclei at different latitudes indicate that the interaction cross section is energy insensitive and is smaller than geometric. Curves are presented showing the ratio of the secondary light element (Li, Be, B) flux relative to the medium element ($6 \leq Z \leq 10$) flux as a function of atmospheric depth.

INTRODUCTION

THE heavy primary component of the cosmic radiation consists of nuclei with charges ranging from $Z=3$ to $Z \sim 26$.¹ The flux of these nuclei is small in comparison to the proton and α -particle flux (~ 1 percent of the proton flux) and increased statistics can be obtained by studying the behavior of various charge groups rather than that of individual charged nuclei. In

the following discussion three different charge groups will be referred to: (1) *L*, light nuclei, $3 \leq Z \leq 5$, (2) *M*, medium nuclei, $6 \leq Z \leq 10$, and (3) *H*, heavy nuclei, $Z > 10$.

In its passage through the atmosphere the heavy primary component changes in character since some particles are lost from the beam because of interaction and ionization loss while others are added to the beam as fragmentation products of interactions of nuclei of higher charge. Since the interaction mean free path of heavy nuclei in atmosphere is quite short (~ 20 to 40 g/cm²) direct measurements on the chemical composition must be made at extremely high altitudes. At the balloon altitudes attained on most experiments dealing with the heavy nuclear component of the cosmic radia-

* This research was supported in part by the United States Air Force through the Office of Scientific Research, Air Research and Development Command.

¹ For a review of the situation as of 1951 see the article by B. Peters in *Progress in Cosmic Ray Physics*, edited by J. G. Wilson (North Holland Publishing Company, Amsterdam, 1952), Vol. I. A survey covering results as of the fall of 1953 is given by E. P. Ney in the Report of the Duke Conference on Cosmic Radiation (unpublished).

tion (~ 10 to 30 g/cm² of residual atmosphere) passage through the residual atmosphere has caused an appreciable adulteration of the incident beam; as a result of these difficulties, *viz.*, a relatively small incident flux and observations under finite amounts of absorber, the true relative flux values at the top of the atmosphere for the three charge groups have not been definitely established. This work was carried out in an attempt to determine more precise values for those parameters involved in the diffusion of the heavy nuclei through atmosphere.

Interactions of heavy nuclei with target nuclei of photographic emulsion have been examined and the fragmentation products from interactions in gelatin and cellulose acetate have also been studied. From this data we have derived the interaction mean free paths and the fragmentation probabilities for the medium and heavy nuclei in atmosphere and calculations have been made to estimate the secondary light element flux at different depths in the atmosphere. By working at two different latitudes, 41° and 55° geomagnetic, information has been gained about the energy dependence of these parameters.

EXPERIMENTAL DETAILS

Three stripped emulsion stacks were used in this experiment. In each case the stripped emulsions (manufactured by Ilford Ltd.) were 4 in. \times 6 in. \times 400 μ and were mounted on glass after exposure and before processing. The development was by the usual temperature methods, and after completion each plate was cut into four 3 in. \times 2 in. sections for microscopic observations.

Two of the stacks, the *C* and *SG* stacks, were flown at White Sands, New Mexico ($\Lambda = 41.7^\circ$, cutoff energy = 1.5 Bev/nucleon) and the third stack, the *SM* stack was flown at Minnesota ($\Lambda = 55^\circ$, cutoff energy = 0.31 Bev/nucleon). The *C* stack contained ninety-two 400 μ *G-5* stripped emulsions arranged horizontally with thin tissue paper between successive emulsions. The flight was for ~ 9 hours at ~ 92 000 ft. The emulsions in this stack were not aligned. The *SG* stack consisted of 19 triads of *G-5*, *G-5*, *G-0* (200 μ each) combination emulsions, and 400- μ gelatin sheets. All members were in direct contact and the stack was aligned after processing. It was flown with vertical geometry for ~ 9 hours at an altitude varying from 97 000 ft to 70 000 ft. The *SM* stack consisted of two parts. Part *A* contained 11 triads of *G-5*, *G-5*, *G-0* combination emulsions, and 400- μ cellulose acetate sheets. Part *B*, in contact with *A*, contained 23 400- μ *G-5* emulsions. All emulsions were in direct contact and the stack was flown vertically for ~ 8.2 hours at ~ 92 000 ft. After processing this stack was aligned for easier tracing.

CHARGE CALIBRATION AND SELECTION CRITERIA

Selection of tracks in scanning in this experiment was done on the basis of δ -ray density. The number of δ rays

per unit length $n_\delta(Z) = Z^2 F(\beta)$, where Z = the charge of the particle and βc its velocity. At relativistic velocities, $\beta \approx 1$, $F(\beta)$ is constant so that n_δ is directly proportional to Z^2 . At 41° geomagnetic latitude almost all particles are at sufficiently relativistic velocities so that in most cases the observed δ -ray density is a direct measure of their charge. However at 55° this does not hold since a large majority of the nuclei are nonrelativistic, and exact charge identification requires a measure of the velocity as well as of δ -ray density. One method of charge determination is to combine measurements of δ -ray density with multiple Coulomb scattering. This, however, imposes severe geometrical limitations on the acceptability of tracks since very long tracks (≥ 3 mm/emulsion) are required for scattering measurements, and the number of acceptable tracks is thus severely limited. For this reason this method of charge identification was not used in this experiment (except for a few tracks in the *SM* stack).

The method adopted for charge identification involved the simultaneous measurement of δ -ray density and range, the latter being a measure of velocity. The observed δ -ray density for a track establishes an upper limit for the charge: since $F(\beta < 1) > F(1)$, we obtain a maximum estimate for the charge of a given track by assuming that it is relativistic, $Z_{\max}^2 = n_\delta$ (observed)/ $F(1)$. In addition each track is observed in the stack for some finite range R and since its actual velocity $\beta > \beta(R)$, a minimum estimate for the charge is obtained as $Z_{\min}^2 = n_\delta$ (observed)/ $F(\beta(R))$. The error in charge determination $\Delta Z = Z_{\max} - Z_{\min}$ obtained in the above manner is a function of the observed range R of the track and varies from $\Delta Z = 3$ for $R = 10$ g/cm² to $\Delta Z = 1$ for $R = 30$ g/cm². In practice a better estimate than this can be accomplished by observing the variation of δ -ray density with range. δ -ray counting can be done with sufficient statistical accuracy to detect variations of < 10 percent in δ -ray density. For nuclei having an energy per nucleon $\epsilon \geq 0.8$ Bev, the δ -ray density is sufficiently constant and β close enough to 1 so that the observed n_δ is a direct measure of charge. Nuclei which have $\epsilon < 0.8$ Bev will change in δ -ray density by > 10 percent in a range $R \sim 15$ g/cm². To consider a specific example: a boron nucleus with the same δ -ray density as a relativistic carbon would change its δ -ray density by ~ 12 percent in 15 g/cm², a beryllium nucleus would change by ~ 36 percent in the same range and lithium nucleus would have a range of only 7.5 g/cm²; similar results obtain for higher charged nuclei. It is thus possible by observing the variation of δ -ray density with range (for $R \sim 15$ g/cm²) to establish the charge within one unit. For our experimental conditions this situation was realized in most cases. For those cases in which the observed δ -ray density was constant within the statistical accuracy the higher charge (Z_{\max}) was assigned, while for the opposite case a charge of $Z_{\max} - 1$ was assigned. The variation of δ -ray density with range used in this experiment was derived from the Bristol calibra-

tion² which gave δ -ray density as a function of velocity. Verification of this relationship has been recently obtained independently by Tidman *et al.*³ on both a theoretical and an experimental basis.

Charge calibration was established by studying fast α particles and heavier fragments from interactions of fast heavy nuclei. Some measure of the energy of the incident heavy nucleus can be obtained from the degree of collimation of the fragmentation products. Relativistic α particles are easily distinguished by their grain density and thus measurements can be made on the opening angles of the α particles in the fragmentation products. Kaplon *et al.*⁴ have shown that the root-mean-square angle which these shower particles make with the direction of the incident primary in the laboratory system is $(\theta^2)^{1/2} = 0.056/E$, where E = total energy in Bev of the incident nucleus. As examples, for a nucleus with $\epsilon = 1$ Bev and $A = 14$ this angle is $\sim 1.8^\circ$ and for a nucleus of $A = 31$ the angle is $\sim 1.3^\circ$.

Fast α particles (selected by grain density) from interactions of fast heavy nuclei were δ -ray counted over large distances to obtain satisfactory statistics. This allows one in first order to predict the δ -ray density for fast nuclei of arbitrary charge. This can be checked by studying stripping reactions of heavy nuclei in which charge balance can be obtained between the incoming primary and the outgoing jet of fast fragments. Figure 1 shows an example of a suitable interaction for calibration purposes. In this reaction a fast carbon nucleus interacts to produce as fragmentation products a lithium nucleus, an α particle, and a proton: the charges of all particles involved can be established unambiguously. By studying reactions of this type it was possible to deduce the δ -ray density for a relativistic singly charged particle $n_\delta(1)$ and the background b by using the relation $n_\delta'(Z) = Z^2 n_\delta(1) + b$.⁵ In our experiments we used a 4-grain convention in δ -ray counting and reduce our observed δ -ray counts to the number observed per 100μ . For the quantities $n_\delta(1)$ and b we found 0.078 and 0.22 for the *C* stack, 0.106 and 0.06 for the *SG* stack, and 0.097 and 0.1 for the *SM* stack. The background contribution b is a function of the length of time between manufacture of the emulsion and subsequent development after exposure. The difference between the value of $n_\delta(1)$ for the *C* stack and that for the *SG* and *SM* stacks is probably due to the geometry. Since the emulsions in the *C* stack were flown horizontally, the average track length is much shorter than that in the other two stacks which were flown vertically: the difference is thus a reflection of the adoption of different acceptance criteria for δ rays. δ -ray counting, however, could be done consistently in all stacks and calibration

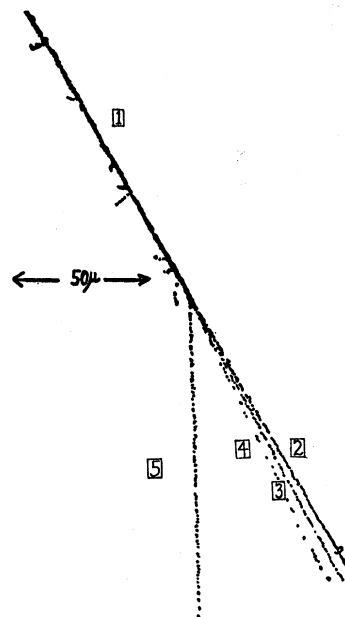


FIG. 1. A carbon nucleus (1) interacts with hydrogen of the emulsion giving a lithium nucleus (2), an α particle (3), and a proton (4). The recoil proton (5) is clearly visible at a wider angle.

tracks in each stack showed variations of less than 5 percent in different emulsions.

The *G-0* emulsions in this experiment were used mainly to obtain increased statistics (by grain counting) over that obtained by δ -ray counting for charge determination of α particles and the lighter elements ($Z \leq 6$).

The following scanning criteria were adopted. For the vertical emulsions, the *SM* and *SG* stacks, all tracks with projected length $> 750\mu$ and $n_\delta \geq 2$ in the survey plate were accepted. For the horizontal stack, the *C* stack, all tracks with projected length $> 450\mu$ and $n_\delta \geq 3$ in the survey plate were accepted. All tracks satisfying the selection criteria were then systematically traced through the stack, either to an exit point or to an interaction. Those slow singly and doubly charged particles which satisfied the acceptance criteria were easily rejected on a range basis. The acceptance criteria for the *SM* and *SG* stacks certainly ensured the inclusion of all nuclei with $Z \geq 6$, though in the *C* stack some nuclei of charge 6 may not have been accepted. However, any lack of 100 percent acceptance efficiency in no way affects the results of this experiment with respect to the interaction mean free paths and fragmentation probabilities.

INTERACTIONS IN EMULSION

214 interactions of heavy nuclei in emulsion were analyzed with respect to the fragmentation products, which are collimated in the direction of the incident primary, and the number of star prongs of the target nucleus, N_h , which includes all gray + black tracks. The results are given in Table I. In this table the interactions

² Dainton, Fowler, and Kent, *Phil. Mag.* **43**, 729 (1952).

³ Tidman, George, and Herz, *Proc. Phys. Soc. (London)* **A66**, 1019 (1953).

⁴ Kaplon, Peters, Reynolds, and Ritson, *Phys. Rev.* **85**, 295 (1952).

⁵ $n_\delta'(Z)$ is the experimentally measured δ -ray density; $n_\delta(Z)$, the true observed δ -ray density, is given by $n_\delta(z) = n_\delta'(z) - b$.

and their products are divided according to the latitude of the flight. The primary nucleus is listed and under each primary nucleus is listed the resultant products and the number of star prongs (N_h). In some interactions charge balance was not obtained between the outgoing jet of fragments and the charge of the primary. These involve meson production and will be discussed later; for these cases the number of protons listed in Table I is that number required to give charge balance. Examples of different types of interactions are given in Figs. 1, 2, and 3. Events in which a (—) occurs are ones in which no information could be obtained on the interaction fragments, either because they were indistinguishable from star prongs or because the interaction was geometrically located so that it was impossible to study it in detail and determine the charge of the fragments.

Three separate classes of particles can be seen to result from interactions of heavy nuclei with target nuclei of the photographic emulsion.

(1) Fragmentation products, both singly and multiply charged, arising from the incident nucleus and collimated in the forward direction (the degree of collimation depending on the velocity of the incident primary).

(2) Light and gray shower tracks also emitted in the forward direction but less strongly collimated than the nuclear fragments of (1).

(3) Evaporation prongs and recoil nuclei generally of short range and roughly isotropic in distribution. These three classes of particles can be understood as follows. In an interaction of a fast nucleon with a target nucleus of the photographic emulsion, particles in the second and third classes are observed to be produced. The interaction of a heavy nucleus with a target nucleus of the emulsion can be considered as a superposition of

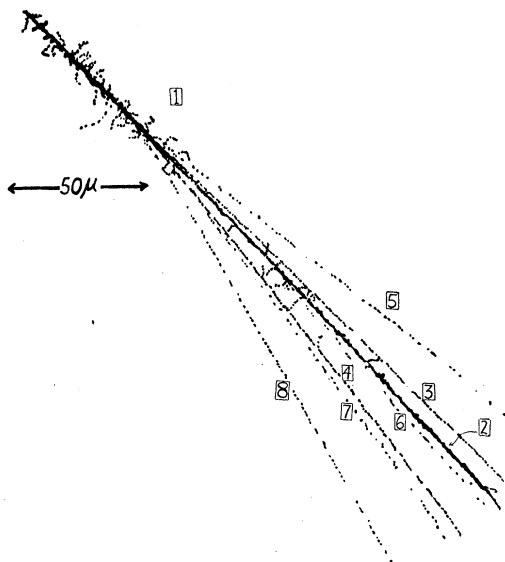


FIG. 2. An argon nucleus (1) interacts with a hydrogen nucleus of the emulsion giving a sodium nucleus (2), two α particles (3) and (4), and three protons (5), (6), and (7). The recoil proton track is track (8).

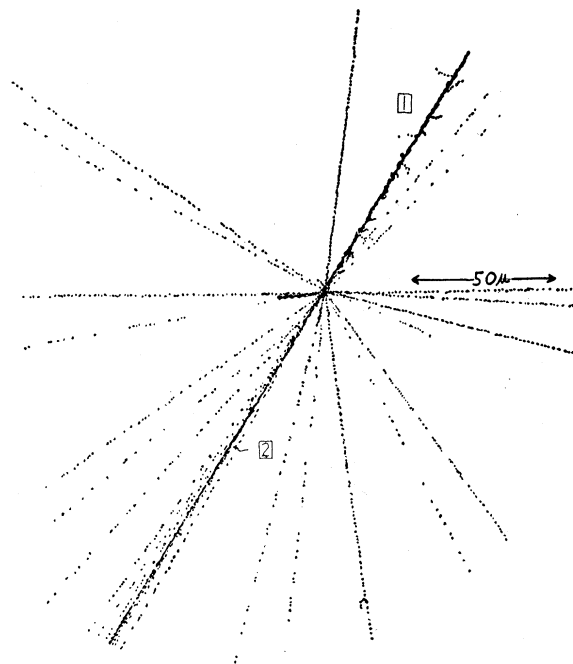


FIG. 3. A fluorine nucleus (1) interacts with a heavy nucleus of the emulsion (probably silver) and produces a lithium nucleus (2), and six protons. The target nucleus gives an evaporation star.

many nucleon-nucleon collisions resulting in the production of particles of the second and third classes. In addition, in the rest system of the incident nucleus, particles of the third class will be produced which will appear in the laboratory system as the jet of fast singly and multiply charged particles collimated in the direction of the incident primary; the relatively small opening angle of the jet is a reflection of the low emission velocity of these particles in the rest system of the incident nucleus.

The photographic emulsion consists of both heavy and light elements; the average atomic weight A of the heavy elements in the emulsion is ~ 84 and that of the light elements (excluding hydrogen) is ~ 14 . The ratio of geometric cross-sections for the light and heavy elements indicates that $\sim \frac{1}{3}$ of all the interactions should occur with the light elements. If one distinguishes between light and heavy target nuclei on the basis of N_h , characterizing light target nuclei as $N_h \leq 4$ and heavy target nuclei as $N_h > 4$, we find that 0.82 ± 0.11 of all the events are characterized by $N_h \leq 4$. This characterization is the same for both medium and heavy incident nuclei. It would appear then that ~ 20 percent of the interactions with heavy target nuclei result in a small number of star prongs and thus simulate collisions with light target nuclei. It is most likely that interactions of this type are due to edge collisions with the heavy target nuclei. Events characterized by $N_h \leq 4$ will be referred to as L -type events and those with $N_h > 4$ as H -type events.

In Table II we list the fragmentation probabilities

TABLE II. Fragmentation probabilities derived from the heavy primary interactions studied. P_{IJ} = the average number of J type nuclei produced in the interaction of an incident I -type nucleus. Figures for the 41° and 55° flights are listed separately and divided according to the charge group of the primary nuclei. The heavy group represents $Z > 10$ and the medium group $6 \leq Z \leq 10$. H events are those in which $N_h > 4$, L events those in which $N_h \leq 4$. The errors quoted are statistical only.

(a) Medium group: actual ratio of L/H events = $59/72 = 0.82 \pm 0.11$.					
	P_{MM}	P_{ML}	$P_{M\alpha}$	P_{Mp}	
<i>H</i> events					
41°	0.03 ± 0.03	0.22 ± 0.08	1.17 ± 0.19	3.75 ± 0.35	
55°	0.07 ± 0.05	0.13 ± 0.07	1.0 ± 0.18	4.13 ± 0.38	
<i>L</i> events					
41°	0.18 ± 0.08	0.54 ± 0.13	1.0 ± 0.2	1.78 ± 0.25	
55°	—	0.52 ± 0.13	1.9 ± 0.26	1.69 ± 0.24	
<i>L+H</i> events					
41°	0.09 ± 0.04	0.36 ± 0.07	1.09 ± 0.13	2.89 ± 0.19	
55°	0.03 ± 0.02	0.32 ± 0.07	1.44 ± 0.16	2.94 ± 0.22	
$41^\circ + 55^\circ$	0.07 ± 0.02	0.34 ± 0.05	1.26 ± 0.1	2.91 ± 0.16	
<i>Hydrogen</i> events					
41°	—	0.83 ± 0.37	1.16 ± 0.46	1.0 ± 0.41	
55°	—	0.57 ± 0.28	1.71 ± 0.49	1.0 ± 0.37	
$41^\circ + 55^\circ$	—	0.69 ± 0.23	1.46 ± 0.33	1.0 ± 0.29	
(b) Heavy group: actual ratio of L/H events = $40/49 = 0.82 \pm 0.12$.					
	P_{HH}	P_{HM}	P_{HL}	$P_{H\alpha}$	P_{Hp}
<i>H</i> events					
41°	0.15 ± 0.08	0.23 ± 0.09	0.5 ± 0.14	2.04 ± 0.28	5.2 ± 0.4
55°	0.19 ± 0.1	0.14 ± 0.08	0.19 ± 0.1	2.8 ± 0.37	5.58 ± 0.5
<i>L</i> events					
41°	0.3 ± 0.12	0.2 ± 0.1	0.55 ± 0.17	1.8 ± 0.3	3.95 ± 0.44
55°	0.26 ± 0.18	0.37 ± 0.14	0.37 ± 0.14	2.05 ± 0.34	3.05 ± 0.4
<i>L+H</i> events					
41°	0.22 ± 0.05	0.22 ± 0.05	0.52 ± 0.1	1.93 ± 0.21	4.65 ± 0.31
55°	0.23 ± 0.08	0.25 ± 0.08	0.28 ± 0.08	2.45 ± 0.25	4.37 ± 0.33
$41^\circ + 55^\circ$	0.22 ± 0.05	0.24 ± 0.05	0.41 ± 0.07	2.18 ± 0.15	4.52 ± 0.2
<i>Hydrogen</i> events					
41°	0.2 ± 0.2	0.4 ± 0.28	0.8 ± 0.4	1.8 ± 0.6	5.0 ± 1.0
55°	—	1.0 ± 0.71	—	1.0 ± 0.71	3.0 ± 1.2
$41^\circ + 55^\circ$	0.14 ± 0.14	0.57 ± 0.28	0.57 ± 0.28	1.57 ± 0.48	4.4 ± 0.8

obtained for the interaction of medium and heavy nuclei in emulsion. These probabilities represent the average number of particles of a given type produced per event. The probabilities are given for incident medium and heavy nuclei at the two different latitudes for events classified as L - or H -type events according to the value of N_h , for events classified as interactions with hydrogen nuclei of the emulsion and for all events irrespective of classification.

A consistency check on the fragmentation probabilities can be obtained by evaluating $\bar{Z}_G = \sum_I P_{GI} Z_I$, where Z_I = the charge of the I th type fragment, P_{GI} = the average number of these type fragments produced in interactions of G -type nuclei (either the medium or heavy group) and \bar{Z}_G = an average charge for the group G of heavy nuclei whose interactions are being studied. Evaluation of this sum for \bar{Z}_M and \bar{Z}_H for L , H , and all events independently as a function of latitude gives $\bar{Z}_M = 7.3 \pm 0.3$ and $\bar{Z}_H = 15.4 \pm 0.4$, where the errors encompass the total range of values obtained. In computing these values the *a priori* average Z for the light, medium and heavy nuclei were taken as 4, 7, and 15. These choices were derived from the relative abundances of the different nuclei in each charge group weighted by their interaction cross section. The equality of the

a priori \bar{Z} for a charge group and the calculated \bar{Z} for that group constitutes the desired consistency check.

The general features exhibited by Tables I and II can be understood qualitatively on the basis of the evaporation model (applied in the rest system of the incident nucleus). The most striking feature is the fact that the fragmentation probabilities, P_{ML} and P_{HL} giving the average number of light nuclei produced per interaction of incident medium and heavy nuclei are distinctly larger for L -type events than for H -type events and are quite high (> 0.5) for the hydrogen events. This characteristic strongly suggests that the lighter the target nucleus, the higher the probability of obtaining a light nucleus as a fragmentation product of the incident heavy nucleus.

Gottstein⁶ has found some correlation between the charge of fragments and their primaries, *viz.*, that an even-charge primary nucleus tends to give more even- than odd-charge fragments: this correlation was found only for L -type events and for energies > 1 Bev/nucleon. No sign of any such correlation has been found in the interactions studied from all three flights or from L -type events in the stacks flown at 41° geomagnetic latitude.

A total of twenty events were observed which were classified as events occurring with a hydrogen nucleus of the emulsion (see Figs. 1 and 2): these are characterized by an interaction in which the incident heavy nucleus is fragmented and one singly charged track (proton) is observed at an angle appreciably wider than that containing the jet of fast breakup fragments: this track is assumed to be the recoil proton. The relative number of these events found (0.09) is in agreement with the number expected on the basis of geometric cross sections (~ 0.1). In addition to these cases, three other cases have been observed in which the heavy primary nucleus breaks up with no sign of star prongs or visible recoil of a target nucleus and in which charge balance is obtained between the incoming nucleus and its products: three other events of a similar nature have been observed but because of the geometry of the event it is impossible to state definitely that there are no recoil tracks. These six events (the questionable ones are preceded by a ?) are listed in Table III.

Four events have also been observed in which the target nucleus gives a star while the incident heavy nucleus appears to continue on with no loss of charge. Three of these events were observed at 41° , involving incident P, Ca, and Fe nuclei and one at 55° involving an incident Mg nucleus. For the two heavier incident nuclei, Ca and Fe, it is impossible to δ -ray count with sufficient reliability to be sure that one unit of charge was not lost in the interaction, *i.e.*, that a proton stripped from the incident nucleus was the cause of the disintegration of the target nucleus. In the other two cases, however, there is definitely no loss of charge of the incident nucleus in the interaction.

⁶ K. Gottstein, Phil. Mag. 45, 347 (1954).

It seems to us that the two types of events mentioned in the preceding paragraphs i.e., fragmentation without visible recoil, and star production with no loss of charge of the primary, really represent the same physical mechanism, since one can be obtained from the other by a Lorentz transformation. There appear to be two possible explanations for this class of event. The first, and less likely, is to attribute these interactions to Coulomb effects. To estimate this we have considered the decomposition of the Coulomb field into its representative virtual quanta and estimate for our experimental conditions (latitude, flight altitude, charges of nuclei involved, and energy spectrum) the effective mean free path for observing interactions of this type is such that it is very unlikely that more than one of these events could be attributed to this mechanism. The second and more likely assumption is to consider these interactions as initiated by an extended neutron of either the target or incident nucleus. No observable effects in either case would be expected since for those reactions involving interactions with incident nuclei in which no loss of charge occurs, the incident nucleus has long-lived neutron-deficient isotopes (with the exception of Fe) whereas for the other cases (fragmentation with no star prongs) most of the target nuclei of the emulsion have neutron-deficient isotopes that decay by γ emission or by β^+ emission (which could easily be not detected). We believe the latter explanation (extended nuclear structure) represents these events: a situation of this sort is not unexpected in light of recent experiments exploring the nuclear charge distribution.⁷

MESON PRODUCTION

An estimate can be made of the number of fast mesons produced in an interaction where there are collimated light and gray shower tracks in the forward direction. The number of protons among the shower particles is assumed to equal the difference in charge between that of the incident nucleus and the sum of charges in the jet of multiply charged fragments: the remaining light shower tracks are considered to be mesons so that this serves as an upper limit to the number of fast mesons produced (some may be protons from the target nucleus).

In Table IV we list the relative number of events in which meson production occurs and the number of mesons per event. Interactions for the 41° and 55°

TABLE III. Fragmentations observed in which no star prongs or recoil nuclei are seen.

C	\rightarrow	3α
C	\rightarrow	$2\alpha+2p$
N	\rightarrow	$B+\alpha$
(?) ^a Ne	\rightarrow	$B+2\alpha+p$
(?)Na	\rightarrow	$Be+7p$
(?)Mg	\rightarrow	$Ne+1\alpha$

^a Events in which it is impossible to state definitely that there are no recoil tracks are marked (?).

⁷ G. Bernardini and E. L. Goldwasser, Phys. Rev. **94**, 729 (1954).

TABLE IV. Relative number of events in which fast mesons are produced and the number of fast mesons per meson-producing event. The data are divided according to the charge group of the incident nuclei and interactions are classified as *L* events ($N_h \leq 4$) and *H* events ($N_h > 4$).

		Events producing fast mesons	Fast mesons per event
<i>Medium group:</i>			
<i>L</i> events	41°	7/22	5.8 ± 0.8
	55°	1/28	2.0 ± 1.4
<i>H</i> events	41°	25/37	5.2 ± 0.4
	55°	7/28	4.2 ± 0.7
<i>Heavy group:</i>			
<i>L</i> events	41°	4/19	8.7 ± 1.4
	55°	2/18	5.5 ± 1.7
<i>H</i> events	41°	14/23	6.85 ± 0.69
	55°	5/20	3.8 ± 0.9

flights are listed separately and division made according to the charge group of the incident nucleus: *L*- and *H*-type events are listed separately. We have estimated the meson production cross section from the data given here on the basis of a geometrical model. We consider each interaction between nuclei to have occurred with the appropriate median impact parameter⁸ and assume on the basis of uniform nuclear density that all the nucleons in this region contribute to meson production. We thus estimate a lower limit to the meson production cross section, σ (nucleon-nucleon). The observed cross sections (experimentally averaged over the incident energy spectrum) are ~ 6.3 millibarns (nucleon-nucleon) at 55° and 19 millibarns (nucleon-nucleon) at 41° , the median energies for these two flights corresponding to 1.1 and 3.3 Bev/nucleon. These figures can be compared with the nucleon-nucleon total cross section observed at Brookhaven National Laboratory⁹: they find a total *p-p* cross section at 830 Mev of ~ 49 millibarns, and evidence that the cross section thereafter is approximately constant with energy. For the *n-p* cross section at ~ 2 Bev, they find 40 millibarns. At these energies $\sim \frac{1}{4}$ of the total cross section is elastic so that the nucleon-nucleon cross section for meson production is ~ 30 millibarns. Since our estimated cross sections are lower limits to the nucleon-nucleon cross section, they are not inconsistent with the Brookhaven results.

INTERACTION MEAN FREE PATHS

All interactions of heavy nuclei found during the systematic tracing of heavy nuclei were used to measure the interaction mean free path of these particles in emulsion. The observational data and results for the medium and heavy charge groups at the two different

⁸ See section on "Extrapolation to Atmosphere."

⁹ Shapiro, Leavitt, and Chen, Phys. Rev. **95**, 663 (1954); Hill, Coor, Hornyak, Smith, and Snow, Phys. Rev. **94**, 791 (1954).

TABLE V. Interaction mean free paths observed in emulsion for incident medium ($6 \leq Z \leq 10$) nuclei and heavy ($Z > 10$) nuclei at 41° and 55° geomagnetic latitude.

41°	$\lambda_M = 3559/60 = 59.4 \pm 7.8 \text{ g/cm}^2$ $\lambda_H = 1270/37 = 34.7 \pm 5.6 \text{ g/cm}^2$
55°	$\lambda_M = 2229/37 = 60.4 \pm 10.3 \text{ g/cm}^2$ $\lambda_H = 876/22 = 45.5 \pm 10 \text{ g/cm}^2$
$41^\circ + 55^\circ$	$\lambda_M = 59.6 \pm 6 \text{ g/cm}^2$ $\lambda_H = 36.5 \pm 4.8 \text{ g/cm}^2$

latitudes of observation are given in Table V.¹⁰ The flux of particles at 55° with energies between 0.31 (cutoff) and 1.5 Bev/nucleon is ~ 4 times the flux of particles with energies > 1.5 Bev/nucleon (cutoff at 41°) so that by comparing the interaction mean free paths at 55° and 41° one can gain some information on the energy dependence of the mean free path, λ . From the experimental results λ seems substantially independent of energy, for energies at least as high as ~ 6 Bev/nucleon (30 percent of the nuclei at 41° have $\epsilon > 6$ Bev).

The mean free path can be written as $\lambda = 1/(\sum_i n_i \sigma_i)$, where n_i = the number of atoms/cc of the different emulsion target nuclei and σ_i = the interaction cross section for the i th type nuclei in the emulsion. If one calculates the mean free path λ by using the known emulsion composition and the cross section given by $\sigma_i = \pi(R_i + R_{inc})^2$, where $R = r_0 A^{1/3}$, ($r_0 = 1.45 \times 10^{-13}$ cm) it is found that the values obtained for λ are much shorter than those observed, or in other words, the observed cross section is smaller than that predicted by a purely geometrical model. The indication is therefore that either nuclei are somewhat transparent, or that the measure of the nuclear radius (r_0) given above is too large.

The experimental data can be fitted in three ways: (1) by using a smaller value for r_0 ; (2) by requiring some overlap of the nuclear volumes to occur before an interaction can take place¹¹; (3) by considering the transparency of nuclear matter. The first two methods will be discussed below. Method (3) has been considered in detail by Eisenberg¹² in a recent paper.

An average Z has to be chosen for both the medium and heavy charge groups of the incoming heavy nuclei. For the medium charge group an average Z , $\bar{Z} = 7$ and for the heavy group $\bar{Z} = 15$, have been obtained by considering the 214 interactions where the primary charges have been established and weighting the relative numbers of incident nuclei by their respective interaction cross-sections. This gives the true relative fluxes of the individual nuclei and allows one to estimate an

¹⁰ The interaction mean free path for L nuclei (λ_L) was found to be $61.7 \pm 19.4 \text{ g/cm}^2$; this value was obtained from interactions of L nuclei in a study of a limited number of long tracks in part B of the SM stack.

¹¹ H. L. Bradt and B. Peters, Phys. Rev. 77, 54 (1950).

¹² Y. Eisenberg, Phys. Rev. 96, 1378 (1954).

average charge to represent the medium and heavy groups which were sampled to obtain the interaction mean free paths. If one now tries to fit the experimental data for the interaction mean free path by varying r_0 it is found that a value of $\sim 1.0 \times 10^{-13}$ must be chosen for the medium group and a value of $\sim 1.1 \times 10^{-13}$ for the heavy group. The value of r_0 depends on the value of \bar{Z} chosen but is not sensitive to a change of one in \bar{Z} .

The second procedure requires that some overlap (ΔR) of the nuclear radii occur before an interaction takes place, so that the available cross section is reduced. The value of $\Delta R = 0.85 \times 10^{-13}$ cm found by Bradt and Peters¹¹ for interactions in glass will give good agreement with the observed data for interactions in emulsion. The interaction cross section for the i -th emulsion constituent is given by $\sigma_i = \pi(R_i + R_{inc} - \Delta R)^2$, where the symbols have the same meaning as before, and the same value of r_0 is used. We find $\lambda_M = 56.5 \text{ g/cm}^2$ and $\lambda_H = 36.5 \text{ g/cm}^2$ to be compared with the experimental values of 59.6 and 36.5, respectively.¹³

This procedure seems preferable since method (1) would predict a nuclear density varying with mass number. We have adopted this procedure [method (2)] to extrapolate our results to atmosphere.

EXTRAPOLATION TO ATMOSPHERE

The interaction mean free paths for the medium and heavy groups were extrapolated to atmosphere by using method (2) and the value of ΔR adopted in the above paragraph. We obtain $\lambda_L = 31.5 \text{ g/cm}^2$, $\lambda_M = 26.5 \text{ g/cm}^2$ and $\lambda_H = 18.0 \text{ g/cm}^2$. These figures are in agreement with those inferred from the measurements in glass by Bradt and Peters.¹⁴ The values measured in glass are not interaction mean free paths but most probably represent a value lying between that of an interaction and an absorption mean free path since interactions occurring in glass involving a loss of one or two units of charge may easily be missed. The value deduced for λ_H in atmosphere is in agreement with the measurement of Freier *et al.*¹³ at 30° geomagnetic latitude from observations on the angular distribution. They find a value in air of $\lambda_H = 21 \pm 2 \text{ g/cm}^2$: this is an attenuation mean free path and should therefore be of the order of $\lambda_H/(1 - P_{HH}) = 24 \text{ g/cm}^2$.

The various fragmentation probabilities found in emulsion can also be extrapolated to corresponding figures for atmosphere. The experimental data for hydrogen and L -type events show increased fragmentation into light elements and a decrease in the number of protons per interaction. It seems reasonable that in a glancing collision the incoming nucleus will not receive as much excitation as in a more direct collision with a target nucleus. In the latter type of collision one would expect rather complete disintegration, while in a glancing collision there seems a greater probability for

¹³ Freier, Anderson, Naugle, and Ney, Phys. Rev. 84, 322 (1951).

¹⁴ H. L. Bradt and B. Peters, Phys. Rev. 80, 943 (1950).

the occurrence of heavier fragments since there will not be as much chance of energy being distributed among the constituent nucleons. This suggests that it is the amount of overlap of the nuclear radii which determines the fragmentation probability in an interaction; the more complete the overlap, the more complete the disintegration of the incoming nucleus.

For collisions between two nuclei, the impact parameter x will have possible values between 0 and D , where D = the maximum distance between the centers of the two nuclei at which an interaction can take place: $D = R_1 + R_2 - 2\Delta R$. Since all collisions are assumed to occur with impact parameters lying between these limits, the probability of an interaction occurring $P = K \int_0^D x dx = 1$, where K is the normalization constant. The probability of an interaction with an impact parameter between D and $D-d$ is given by $P_d = K \int_{D-d}^D x dx = [D^2 - (D-d)^2]/D^2$ (see Fig. 4). For smaller target nuclei, i.e., smaller D , the proportion of collisions with impact parameters between D and $D-d$ increases. For a fixed incoming nucleus (as example we consider an incident-heavy nucleus) it is reasonable to assume that collisions with impact parameters between D and $D-d_H$ yield heavy fragments, between $D-d_H$ and $D-d_M$ medium fragments, between $D-d_M$ and $D-d_L$ light fragments, and for smaller impact parameters (greater overlap) mainly α particles and protons occur.

For smaller target nuclei the proportion of interactions which yield heavy, medium, and light fragments will thus be increased and the number which give α particles and protons decreased. And, as suggested by the interactions in emulsion with light elements, and the glancing collision with heavy elements, the number of protons is reduced most.

The expression for a mixture of target nuclei will be

$$P_d = (\sum_i n_i D_i^2 - \sum_i n_i (D_i - d)^2) / \sum_i n_i D_i^2,$$

where all symbols have been defined previously in the text. The overlap parameters d_H , d_M , d_L can be determined to fit the observed probabilities P_{HH} , P_{HM} , and P_{HL} (here we specify an incident heavy nucleus) in emulsion: these are then used with the known composition of air to determine the fragmentation probabilities for that medium. The results obtained for atmosphere for both incident medium and heavy nuclei are given in

TABLE VI. Fragmentation probabilities derived for incident medium- and heavy-nuclei interactions in air. The corresponding fragmentation probabilities observed in emulsions for L type events (averaged for 41° and 55° geomagnetic latitude are listed for comparison).

	Air (derived)	Emulsion (L events)		Air (derived)	Emulsion (L events)
P_{HH}	0.25	0.28			
P_{HM}	0.27	0.24	P_{MM}	0.13	0.18
P_{HL}	0.48	0.45	P_{ML}	0.42	0.53
$P_{H\alpha}$	2.07	1.9	$P_{M\alpha}$	1.42	1.40
P_{Hp}	4.29	3.45	P_{Mp}	1.70	1.73

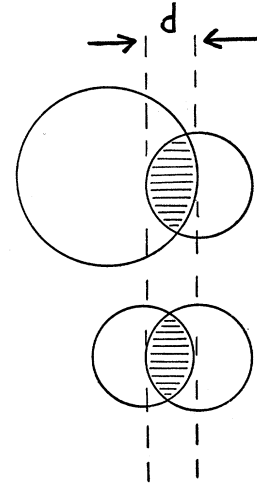


FIG. 4. This figure illustrates collisions between an incident heavy nucleus and target nuclei of different size. Though the overlap d is the same in both cases, for smaller target nuclei proportionately more of the effective cross section is utilized than for larger target nuclei.

Table VI. The values for the α particle and proton fragmentation probabilities are derived by requiring that $\bar{Z}_I = \sum_I P_{II} Z_I$ and that $P_{I\alpha}/P_{Ip}$ have the same value as for the L -type events observed in emulsion.

An experimental check on the fragmentation probabilities listed for atmosphere in Table VI was obtained by studying the fragmentation products emitted in the interactions of heavy primary nuclei with the target nuclei of cellulose acetate and gelatin (each of these consists of only light elements, C, N, O, and H). The sandwich emulsion and absorber stacks only allow one to examine the fast fragments carrying on in the direction of the incident primary, not the interaction itself. Since the absorber sheets are approximately equal in thickness to the emulsions used, the geometry is good and it is not likely that fragments at wide angles (see Fig. 2) will be missed (work done with emulsions mounted on glass suffers from the disadvantage that wide-angle fragments could be easily missed in scanning the next emulsion). Since the density of the plastic is low, only a limited number of interactions were found and statistics are not sufficient to give very definite results. We have combined our results for the fragmentation probabilities observed at both latitudes in Table VII. It is seen that these are, within statistics, in agreement with the fragmentation probabilities derived for atmosphere (approximately equivalent in composition with respect to light elements) on the basis of the overlap model. In addition, we note that the fragmentation probabilities derived for air are in agreement with those observed for L -type events in emulsion. In the following discussion we shall use the probabilities and mean free paths in atmosphere calculated on the basis of the overlap model.

SECONDARY FLUX OF HEAVY NUCLEI

Observations made on the flux of heavy nuclei at flight altitude under a finite amount of residual atmosphere must be extrapolated to the top of the atmosphere to obtain true primary flux values. In general corrections

TABLE VII. Observed fragmentation probabilities for interactions in light element absorbers of incident medium and heavy nuclei (the data for both latitudes are combined).

$P_{MM}=0.06\pm 0.06$	$P_{HH}=0.16\pm 0.16$
$P_{ML}=0.35\pm 0.14$	$P_{HM}=0$
$P_{M\alpha}=1.59\pm 0.39$	$P_{HL}=0.83\pm 0.37$
$P_{Mp}=2.7\pm 0.66$	$P_{H\alpha}=1.66\pm 0.55$
	$P_{Hp}=5.5\pm 2.2$

must be made for loss by ionization and interaction, and for the proportion of the observed flux which is secondary in origin. The most appropriate way to correct for these effects is to consider the diffusion of the heavy nuclei component in the atmosphere. We assume parallel beams of nuclei travelling through the atmosphere and neglect ionization loss: in addition in interactions of heavy nuclei we assume the fragmentation products maintain the same direction and the same energy per nucleon as the primary. The diffusion equations are:

$$dN_I(x)/dx = -N_I(x)/\lambda_I + \sum_{I' > I} N_{I'}(x)P_{I'I}/\lambda_{I'},$$

$$I, I' = L, M, H,$$

where $N_I(x)$ is the flux of I -type nuclei after passing through x g/cm² of material, $P_{I'I}$ is the probability (assumed energy-independent) in an interaction of an I' nucleus that an I nucleus will be produced, λ_I is the interaction mean free path of an I -type nucleus, also assumed energy-independent, and $x = h/\cos\theta$, where h is the amount of residual atmosphere in the vertical direction and θ is the zenith angle. These equations are subject to the boundary condition $N_I(0) = N_I^0 =$ incident primary flux value for I -type nuclei at the top of the atmosphere. The solutions may be written in the following form:

$$N_H(x) = N_H^0 \exp(-x/\lambda_H'),$$

$$N_M(x) = N_M^0 \exp(-x/\lambda_M') + (\alpha_{HM}P_{HM}/\lambda_H)$$

$$\times [N_H^0 \exp(-x/\lambda_M') - N_H(x)],$$

$$N_L(x) = N_L^0 \exp(-x/\lambda_L') + (\alpha_{ML}P_{ML}/\lambda_M)$$

$$\times [N_M^0 \exp(-x/\lambda_L') - N_M(x)]$$

$$+ (\alpha_{HL}/\lambda_H)(P_{HL} + P_{HM}P_{ML}\alpha_{ML}/\lambda_M)$$

$$\times [N_H^0 \exp(-x/\lambda_L') - N_H(x)],$$

where

$$\alpha_{IJ} = \lambda_I \lambda_J' / (\lambda_J' - \lambda_I') > 0, \quad \lambda_J' > \lambda_I',$$

and

$$\lambda_I' = \lambda_I / (1 - P_{II}).$$

In these equations the first term on the right hand side represents the absorption of a given charge group with the absorption mean free path λ' while the additional terms represent contributions to that charge group by interactions of nuclei of higher charge. The attenuation mean free path, which would be the mean free path measured in atmosphere by observations of flux values as a function of depth would be depth de-

pendent and is properly defined by $-dN_I(x)/dx = N_I(x)/\lambda_I^{Att}$.

It is in general difficult to make a calculation which can be applied to all observational cases, since in general the zenith angles accepted and the geometrical acceptance factor depend on the particular experiment. We have thus calculated the observed fluxes (for parallel incident beams) at various depths in the atmosphere assuming different values for the relative incident fluxes. Since the medium element flux is the highest, the light and heavy fluxes are expressed in terms of it. In Fig. 5 we have plotted two different sets of curves relating the light and medium element fluxes. The lower family of curves gives the ratio of secondary light element flux to medium flux $[N_L^{sec}(x)/N_M(x)]$ at a depth x for different values of the fragmentation probabilities and of the ratio of incident medium and heavy fluxes: Curves I and II are calculated with $P_{ML}=0.42$ and $P_{HL}=0.48$ and values of $R_{HM}=N_H^0/N_M^0$ of 0.5 and 0.33, respectively, while Curve III is calculated with $P_{ML}=P_{HL}=0.23$ (the value used by Bradt and Peters,¹⁴ and

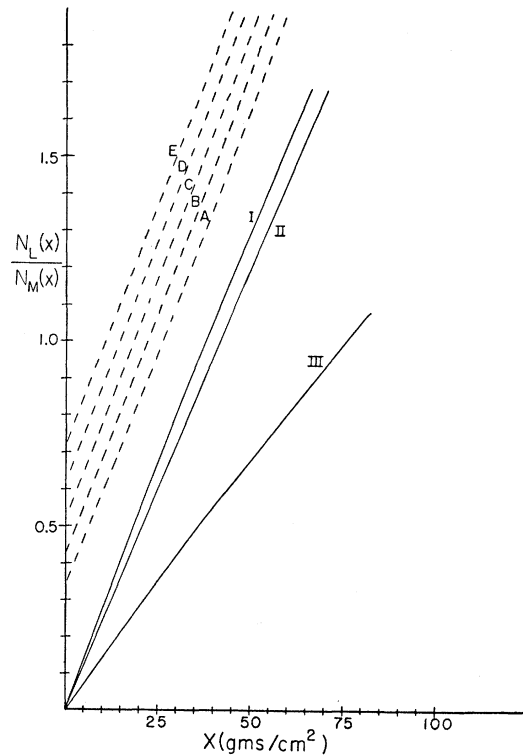


FIG. 5. Curves I, II, III represent the relative secondary light element flux $N_L(x)/N_M(x)$ versus path length in the atmosphere; the following parameters were used.

$$\begin{array}{lll} \text{I:} & P_{ML}=0.42, & P_{HL}=0.48, \quad R_{HM}=0.5. \\ \text{II:} & P_{ML}=0.42, & P_{HL}=0.48, \quad R_{HM}=0.33. \\ \text{III:} & P_{ML}=0.23=P_{HL}, & R_{HM}=0.5. \end{array}$$

Curves A, B, C, D, E represent for assumed incident ratios of light to medium elements ($N_L^0/N_M^0=0.3$ for A in increments of 0.1 up to 0.7 for E) the relative observed light-element flux $N_L(x)/N_M(x)$ versus path length in the atmosphere, if one uses the parameters of Curve I.

Dainton *et al.*²) and $R_{HM}=0.5$. The upper curves, *A* to *E*, represent the observed ratio of light-element flux to medium-element flux at a depth x if one uses the parameters of Curve I and assumes a ratio of light to medium incident flux, $R_{LM}=N_L^0/N_M^0$, of 0.3, 0.4, 0.5, 0.6, 0.7, respectively for the curves *A* to *E*. Thus from an observed ratio of light to medium flux at a given depth, the ratio at the top of the atmosphere can be read off directly from curves *A* to *E*. These results are not sensitive to variations of ~ 10 percent in the mean free paths.

The attenuation length for the medium-element group varies from 38 g/cm² at the top of the atmosphere to 30.4 g/cm² at infinite depth. Because of our choice of only three charge groups, the attenuation length for the heavy nuclei is equal to the absorption length (24 g/cm²), which is in agreement with Minnesota results.¹³

RELATIVE ABUNDANCES

The observed number of interactions of the individual charged nuclei within each charge group weighted by their individual interaction cross sections allows one to make an estimate of the ratio of the heavy and medium charge groups observed at a given depth and represents a lower limit to that ratio at the top of the atmosphere since the heavy group is attenuated more strongly than the medium. The figure deduced from the 214 interactions observed¹⁵ is $R_{HM}=0.5$. This figure is in agreement with that of Gottstein⁶ who obtained $R_{HM}\sim 0.6$ from a study of the interactions of heavy nuclei. From the results of different laboratories^{1,11,13,16} of the direct measurement of the heavy-element flux, R_{HM} could lie between 0.33 and 0.5. Application of this same method also allows one to obtain some idea of the abundance of different elements within a given charge group. In an estimation of this type, as well as that made above, some distortion is introduced at high latitudes because of ionization loss in the residual atmosphere. From our results we can make the following qualitative statements. The abundance of nitrogen is greater than that of oxygen while the carbon and nitrogen abundances seem of comparable magnitude. There is no indication

¹⁵ We estimate that the loss of carbon nuclei in the *C* stack due to the high δ -ray acceptance criterion, will affect our relative abundances by $<10\%$.

¹⁶ Kaplon, Noon, and Racette, Phys. Rev. 96, 1408 (1954).

that, for particles with Z between 8 and 14 inclusive, nuclei of even charge are 3 times as numerous as those of odd charge as suggested by the Bristol results.² For 104 interactions involving incident nuclei in this charge group, the ratio of odd/even nuclei is found to be ~ 1.0 .

CONCLUSIONS

The interaction mean free paths in emulsion have been measured for the medium and heavy charged nuclei at geomagnetic latitudes 41° and 55°. It has been found that the mean free paths are independent of the latitude of measurement and therefore of energy, for energies up to ~ 6 Bev/nucleon. The cross sections implied by the observed mean free paths in emulsion are smaller than geometric. The data have been fitted by using a simple geometrical model requiring an overlap of the incident and target nuclei before an interaction occurs.

The interactions observed in emulsion show a high probability for the production of light elements in the interactions of medium and heavy nuclei, the probability being greatest for smaller target nuclei. The results observed in emulsion have been extrapolated to atmosphere and fragmentation probabilities derived for incident medium and heavy nuclei. These probabilities are in agreement with experimental observations on interactions occurring in an absorber consisting mainly of C, N, O, and H and with *L*-type events in emulsion. Curves are presented showing the contribution of interactions in the residual atmosphere to the flux of light nuclei as a function of depth.

Information has been obtained about the relative abundances of the heavy primary nuclei. C and N are observed to be of comparable magnitude, while O is less than either of these. The ratio of heavy to medium nuclei at the top of the atmosphere is estimated to be ~ 0.5 . No evidence is obtained for a predominance of nuclei of even charge.

We wish to thank the Aero Medical Field Laboratory of Holloman Air Force Base and the Office of Naval Research for their assistance in obtaining the balloon flights for this experiment. We are indebted to Miss Barbara Hull and Mrs. R. Wargotz for their assistance in scanning and to Miss Phyllis Hull for her assistance both in scanning and with some of the calculations.